Discover Sustainability

RESEARCH

Open Access

Development of Taguchi grey-based hybrid ANFIS prediction model for fused deposition modelling of HIPS

N. Manikandan[1], P. Thejasree[1], Siva Marimuthu[2], Rajadurai Murugesan[3], Bamidele Charles Olaiya[4*] and Awafung Emmanuel Adie[5]

*Correspondence:
Bamidele Charles Olaiya
bmolaiya@kiu.ac.ug
[1]School of Engineering and Technology, Mohan Babu University (MBU), Tirupati, Andhra Pradesh 517102, India
[2]Senior Lecturer in Aeronautical Engineering, Department of Engineering, University of Staffordshire, Stoke on Trent, UK
[3]Department of Aeronautical Engineering, Nitte Meenakshi Institute of Technology, Bengaluru, India
[4]Department of Civil Engineering, School of Engineering and Applied Sciences (SEAS), Kampala International University, Western Campus, Ishaka, Uganda
[5]Department of Biomedical Engineering, Kampala International University, Western Campus, Ishaka, Uganda

Abstract
Fused Deposition Modelling (FDM) is often used in Additive Manufacturing (AM), making it popular for producing even the most complex and tailored geometry forms at low costs. With these advantages, it also has limitations in quality and efficiency in the products made out of it, influenced strongly by process parameters, which necessitate the development of predictive tools for 'control' of the process. This present work emphasizes HIPS material to enhance FDM performance through the establishment of a predictive model using an Adaptive Neuro-Fuzzy Inference System (ANFIS). The three important input variables are infill density (ID), nozzle temperature (NT), and printing speed (PS). The output responses are printing time, dimensional deviation, and surface quality. The experimental matrix is made by using Taguchi's L27 orthogonal array, and therefore, the multiple performance indices from the different responses are derived using Grey Relational Analysis (GRA). These Grey Relational Coefficient (GRC) values obtained from that analysis will then be used as an input variable for training and testing of the ANFIS model. The model evolved from one that had shown good performance in prediction and predicted output responses very well. The model also gives the optimum parameter setting of 25% infill density, nozzle temperature of 240 °C, and printing speed of 65 mm/s for better and improved multiple performance. The findings indicate that the proposed ANFIS-based approach undoubtedly emerges as a strong and effective tool in improving productivity and dimensional precision, as well as overall quality in FDM of HIPS material.

Keywords Additive manufacturing, 3D printing, Fused deposition modelling, Taguchi's design and analysis, Grey theory, Optimization

1 Introduction

Additive Manufacturing (AM) techniques allow a wider class of structures and more complex shapes to be made with the help of geometric data obtained from 3D models. Layer upon layer, material is deposited with this technique. Industries referred to as "AM" include construction, biomedicals, and prototyping. The construction sector has

© The Author(s) 2025. **Open Access** This article is licensed under a Creative Commons Attribution-NonCommercial-NoDerivatives 4.0 International License, which permits any non-commercial use, sharing, distribution and reproduction in any medium or format, as long as you give appropriate credit to the original author(s) and the source, provide a link to the Creative Commons licence, and indicate if you modified the licensed material. You do not have permission under this licence to share adapted material derived from this article or parts of it. The images or other third party material in this article are included in the article's Creative Commons licence, unless indicated otherwise in a credit line to the material. If material is not included in the article's Creative Commons licence and your intended use is not permitted by statutory regulation or exceeds the permitted use, you will need to obtain permission directly from the copyright holder. To view a copy of this licence, visit http://creativecommons.org/licenses/by-nc-nd/4.0/.

been slow to adopt 3D printing, despite its numerous advantages such as waste reduction, design freedom, and automation [1–3]. Novel applications built on advancements in new materials and processes of additive manufacturing (AM) are being developed. The expiration of some earlier patents has been instrumental in reducing barriers to entry into this production method, allowing manufacturers to build their own unique 3D printing machines. Harnessing the fast and cost-efficient prototyping capabilities of 3D printing, architecture and design have largely embraced the technology for developing attractive and functional prototypes [4, 5]. The product development costs are further reduced thanks to 3D printing. Recently, the use of 3D printed parts has increased in many industries, from prototyping to the manufacture of end products. Due to the high costs associated with producing customized items, it was very difficult for manufacturers to meet certain consumer needs. Still, Additive Manufacturing (AM) can exploit 3D printing technology to fabricate customized products cheaply in small batches. This holds significant value in the biomedical sector, where patient-specific solutions are frequently required [6–8].

As depicted in Fig. 1, the FDM method of 3D printing entails creating layers of materials using a continuous filament of a thermoplastic polymer. The filament is heated until it becomes semi-liquid at the nozzle to extrude into a platform or on top of already existing printed layers [9, 10]. Thermoplasticity is one significant property of the polymer

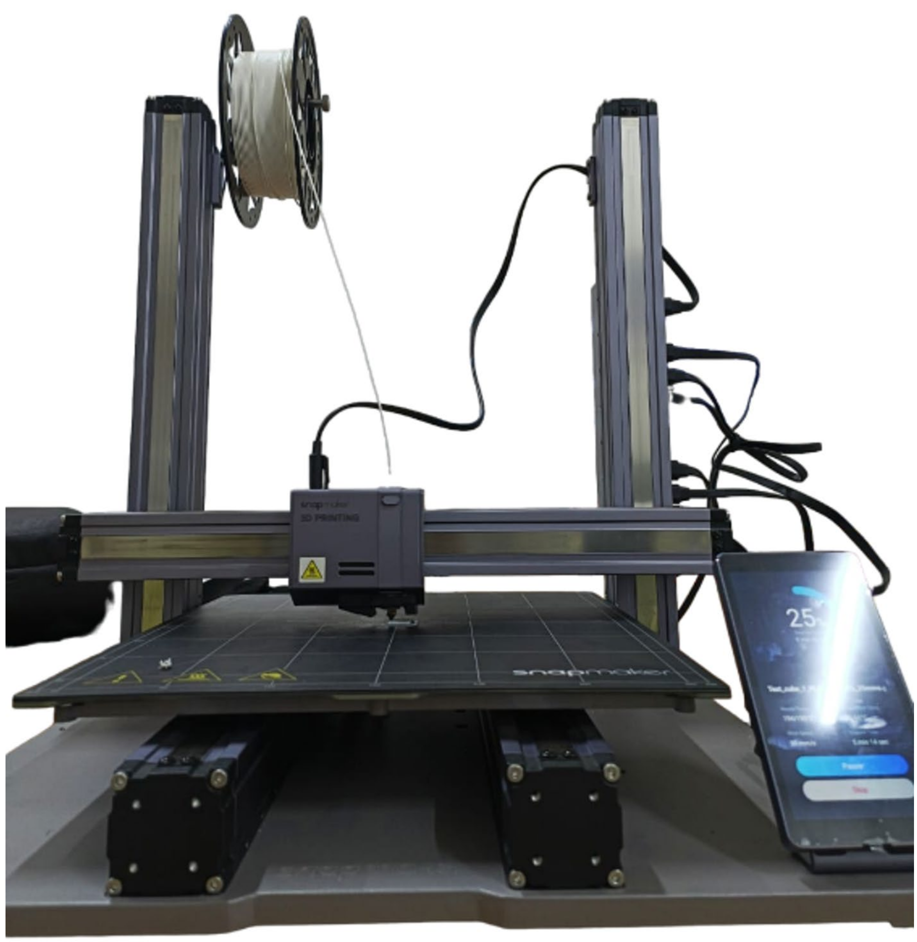

Fig. 1 FDM machine

filament that blends the filaments during printing, and later on, this filament solidifies at room temperature after printing is completed. Printing parameters, many of which determine the mechanical properties, are layer widths, thicknesses, orientations, and air gaps between or within the layers [11, 12]. Inter-layer distortion was then identified to be a major factor causing mechanical weakness. The advantages of FDM are its ease of operation, speed, and relatively low cost. However, the FDM process has shortcomings, including poor surface quality and mechanical properties, visible layer lines, and a limited selection of thermoplastic materials [13]– [14]. To enhance the performance of 3D-printed components, fibre-reinforced composites have been developed through FDM. Nevertheless, achieving proper fibre alignment, developing robust bonds between the matrix and the fibres, and avoiding voids remain major challenges in fabricating high-performance 3D-printed composites [15–17]. Aeronautics, automobiles, medical appliances, electronics, and consumer goods are among the many sectors that depend on FDM-made components. Yet, the mechanical performance limitations of FDM restrict the broader industrial adoption of fabricated products [18, 19]. Since the build settings employed during the process directly affect mechanical properties, careful parameter selection is crucial to maximize performance. Consequently, extensive efforts have been devoted to modelling FDM parameters and optimizing process variables [20].

This growing demand for optimized, sustainable materials in manufacturing aligns with global trends in resource efficiency and circular economy strategies. Recent investigations into waste-derived materials for structural applications have shown promising results in reducing environmental impact while improving material performance. For instance, Olaiya et al. [21–23] demonstrated that banana leaf ash, cassava peel ash, and other agricultural/industrial by-products can be valorized as supplementary cementitious materials, enhancing pozzolanic activity and contributing to sustainable concrete. Similarly, studies on sawdust composites [24] and sandcrete bricks produced from industrial and agricultural waste [25] highlight the potential of integrating low-cost, recycled, and renewable resources into construction materials. These advances underscore how material innovation and optimization, whether in traditional construction or additive manufacturing, can improve mechanical properties while addressing sustainability challenges.

When it comes to FDM, techniques such as the Taguchi method have been applied to optimize process variables for different materials [26–28]. High Impact Polystyrene (HIPS), in particular, has emerged as an adaptable thermoplastic with excellent impact resistance, rigidity, and stability under stress [29, 30]. Its favourable thermoforming, extrusion, and fused deposition modelling characteristics, combined with recyclability and resistance to environmental factors, make it an attractive material for additive manufacturing [31–35]. However, like many thermoplastics, HIPS still faces issues such as porosity, weak interlayer bonding, and anisotropic strength, which necessitate advanced modelling strategies to improve its structural performance [36–39]. Despite numerous optimization studies, most existing approaches rely on conventional statistics or regression models that often focus on single properties, leaving gaps in addressing multi-response objectives, such as printing time, surface roughness, dimensional deviation, and mechanical reliability. In light of this, the present research proposes an Adaptive Neuro-Fuzzy Inference System (ANFIS)-based predictive framework tailored to FDM of High Impact Polystyrene (HIPS), with the dual aim of enhancing process optimization and contributing to the broader discourse on sustainable and efficient material utilization.

In this methodology, key process inputs include nozzle temperature, printing speed, and infill density, whereas output responses are measured in terms of surface roughness, dimensional deviation, and printing time. Grey Relational Analysis (GRA) normalizes and integrates multiple responses into one single Grey Relational Grade (GRG), which is the target for modelling. The ANFIS model is thereby able to learn its internal nonlinear relationship with the unrelated process parameters and combined performance outcomes. So, the proposed approach not only fills the identified gap of limited intelligent multi-response modelling in the case of FDM, but also provides a powerful predictive tool for optimized process control, enhanced product reliability and overall efficiency of additively manufactured components.

2 Materials and methods

The Snapmaker 2.0 is a modular construction system that caters to a whole range of technical applications, considering the following three primary modalities, the most paramount being additive manufacturing through 3D printing. Additive manufacturing employs the Fused Deposition Modelling (FDM) method, one of the most widely accepted techniques of adding material to create 3D objects via extrusion using thermoplastics, layer by layer. Given the majority of the forms of adoption, this acceptance is overwhelmed either in the market of production or in that of consumption, owing to its simplicity, cost-effective nature, and relative ease and convenience in the building of even the most complex geometry. Among the vast range of thermoplastics and the most commonly used FDM materials, HIPS or High Impact Polystyrene is an extremely versatile and typical FDM material. It's a tough polymer synthesized by polymerization wherein styrene monomers are incorporated with additional poly-butadiene for its improved toughness and impact resistance compared to general-purpose polystyrene. It has a comparatively lower melting temperature, good processability, dimensional stability, and excellent resistance to oils, greases, and a variety of chemicals, making it highly suited to thermoforming, extrusion and fused deposition modelling.

HIPS is indeed a material that bears enormous application potential through various industries, mainly due to its non-toxic character, simple workability, durability, impact resistance, and cost-effectiveness. In food packaging, HIPS is used for trays, clamshell containers, blister packs, and storage vessels. In consumer and industrial applications, HIPS is considered an important material in toys, office supplies, electronic housings, and home appliances, where rigidity and dimensional stability are paramount. In the automotive sector, HIPS is also used because of its lightweight and easy processability for instrument panels, trims, and external body parts. The construction industry utilizes HIPS for ceiling tiles, insulation boards, and wall panels where thermal insulation is needed. Its applications in medicine include pharmaceutical diagnostic trays, sample cups, and packaging materials due to its resistance to chemicals and dimensional stability. In the area of additive manufacturing, HIPS is extremely popular in Fused Deposition Modelling (FDM) as an inexpensive and easy-to-handle prototyping material, which can lend itself to post-processing with many methods such as sanding, machining, and painting; hence, it is perfect for functional and end-use components.

Dimensional deviation and surface roughness of the fabricated FDM parts were measured using precision instruments, ensuring an objective basis for performance evaluation. Dimensional deviation, parallelism error and perpendicularity error were assessed by measurement of the actual printed dimensions using a Helmel make Coordinate Measuring Machine (CMM) equipped with a touch-trigger probe, providing an accuracy of ± 2 μm and resolution of 0.5 μm. Surface quality, on the other hand, was assessed using a Mitutoyo SJ210 surface roughness tester with a measurable range of 360 μm with a 0.01-μm resolution on various cut-off lengths from 0.25 mm to 2.5 mm. For a single specimen, surface roughness was measured at different locations, and the average 'Ra' value was considered.

The configuration utilized for FDM is depicted in Fig. 2. Product and process designs may be optimally optimized with the use of the Taguchi Design of Experiments (DOE) approach. To determine how different inputs affect the final result, the Taguchi decision-making process systematically manipulates the inputs at several stages. While taking the possible influence of noise components into account, the main objective is to choose the best combination of input elements that will reduce variation and improve performance. Independent process factors in this study include nozzle temperature (NT), infill density (ID) and printing speed (PS). Printing time, dimensional variation, surface roughness, parallelism and perpendicularity error are the output parameters under consideration.

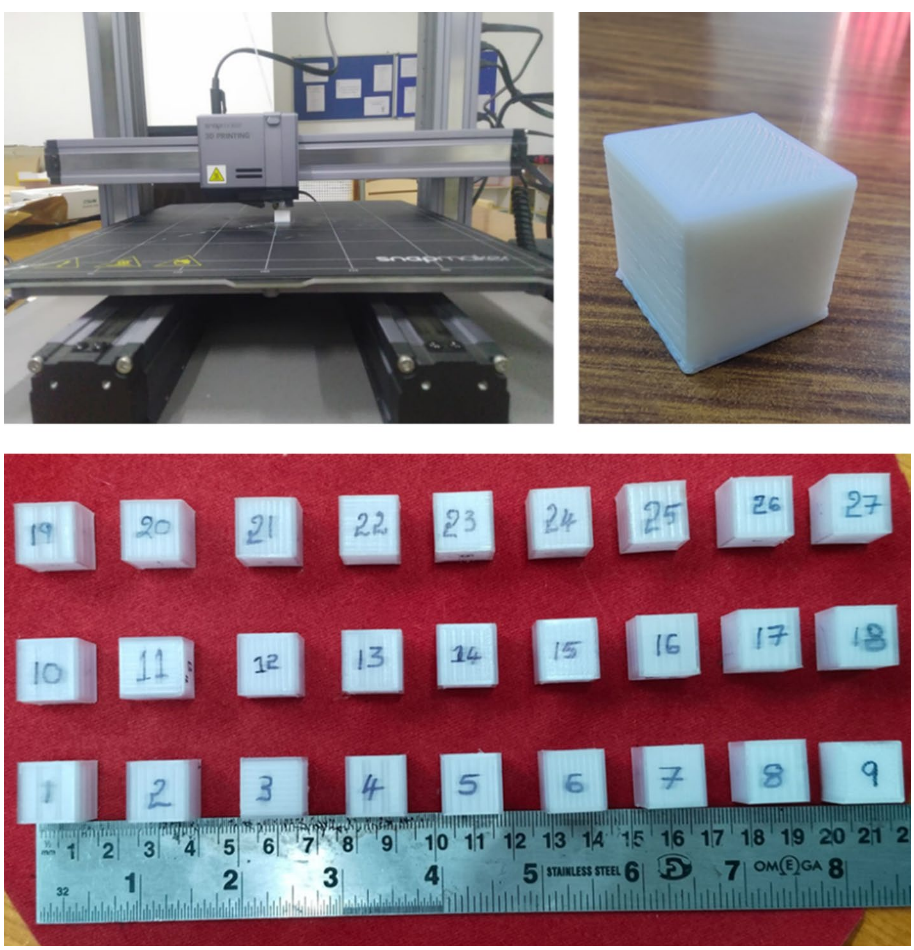

Fig. 2 FDM Setup for experimentation

Among the most important FDM process parameters selected in the study-nozzle temperature, print speed, and infill density-they formed the most consequential parameters that improved the printing performance of the HIPS. The nozzle temperature controls the melt flow, interlayer adhesion and surface finish; print speed governs deposition quality, dimensional accuracy, and printing time; while infill density determines the mechanical properties and overall strength. In preliminary tests, these factors were highly correlated with responses imparting greater justification for their selection.

The levels, ranges, and attributes are depicted in Table 1. Considering the parameters and levels, an L27 orthogonal array has been chosen to perform the tests. For this work, three input factors, nozzle temperature, printing speed, and infill density, were analyzed at three different levels. An L27 orthogonal array was selected to cover all combinations of factor levels extensively and to capture the interaction effects satisfactorily. The design chosen, compared to smaller orthogonal arrays, made provisions for wider space for interactions among factor levels while remaining within the safe operating limits of the HIPS material, making the optimization results more reliable and robust.

2.1 Development of grey-based ANFIS predictive model

Over the past few years, artificial intelligence has greatly shaped the aspects of engineering to allow for the development of modern models and methods for the optimization of many processes. Process control at its finest is essential to improve outcome

Table 1 Input and grey output parameters

Ex. No	Input variables			GRG
	A	B	C	
	Nozzle Temp (°C)	Infill Density (%)	Printing Speed (mm/sec)	
1	230	25	35	0.7690
2	230	25	50	0.6870
3	230	25	65	0.5729
4	230	50	35	0.7108
5	230	50	50	0.6686
6	230	50	65	0.7066
7	230	75	35	0.4542
8	230	75	50	0.5121
9	230	75	65	0.6273
10	235	25	35	0.7372
11	235	25	50	0.7000
12	235	25	65	0.7261
13	235	50	35	0.7138
14	235	50	50	0.6535
15	235	50	65	0.6688
16	235	75	35	0.4961
17	235	75	50	0.5928
18	235	75	65	0.6206
19	240	25	35	0.7908
20	240	25	50	0.7876
21	240	25	65	0.8066
22	240	50	35	0.7612
23	240	50	50	0.7740
24	240	50	65	0.7781
25	240	75	35	0.5721
26	240	75	50	0.6154
27	240	75	65	0.6018

performance results. The exploration of the ANFIS model was made through the supplied data, where the "trapmf" membership function generates rules from the three selected input variables: nozzle temperature, infill density, and printing speed. These rules will then aid in structuring the ANFIS prediction model, taking into consideration all five output responses: surface roughness (SR), dimensional deviation (DD), parallelism error (PRL), perpendicularity error (PERP), and printing time (PT). Let the model predict the properties of parts printed through FDM under all three parameters as well. Figure 3 depicts the ANFIS model editor, while Fig. 4 represents the rule viewer, along with the underlying architecture and the predictions for all five output parameters. This architecture makes comprehensive multi-response prediction possible and provides an accurate means for process optimization of FDM components. The ANFIS model developed in this study follows a multi-input single-output (MISO) framework, which is the structure of the ANFIS model. Specifically, the five Grey Relational Coefficient (GRC) values derived from the measured output responses (surface roughness, dimensional deviation, parallelism error, perpendicularity error, and printing time) were used as the inputs, while the Grey Relational Grade (GRG) was considered as the single output.

Predictive modelling was accomplished using the Adaptive Neuro-Fuzzy Inference System (ANFIS) for its ability to integrate the learning capacity of neural networks with fuzzified reasoning. Taguchi experimental trial data were divided into training and validation sets for the purpose of better generalization and less over-fitting. The ANFIS model utilized a first-order Sugeno-type fuzzy inference system with 'trapmf' membership functions. In this scheme, three membership functions were allotted for each input parameter (nozzle temperature, infill density, and printing speed), making the rule base representative of nonlinear interactions thereof in the process variables.

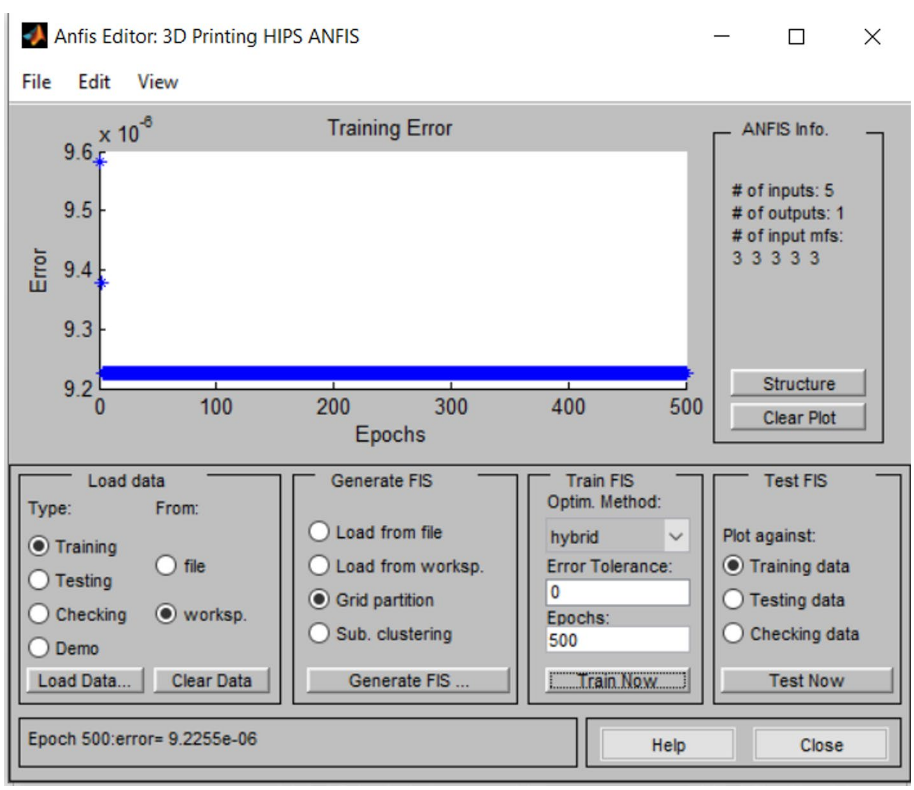

Fig. 3 ANFIS editor

Fig. 4 ANFIS rule viewer

Hyperparameters were selected through an inner iterative testing process, while training was performed on a hybrid optimization algorithm combining Least Squares Estimation (LSE) for consequent parameters and Gradient Descent for premise parameters.

3 Result and discussion

The setup used in the present study for FDM printing of HIPS parts was examined by utilizing an L27 orthogonal array (OA) to determine the effect of various input parameters. The primary objective of this study was to determine the impact of these characteristics on the development of HIPS components. The major objective of the research was to determine the best values for these parameters so that the FDM method might be significantly more successful. Performance is improved when metrics such as Surface Roughness (SR), Printing Time (PT), and Dimensional Deviation (DD) are measured more precisely.

3.1 Optimization of factors on printing time (PT)

Figure 5 depicts the response plot for printing time (PT) for FDM of HIPS material. This investigation establishes a transparent relationship between printing time (PT) and the selected process variables of nozzle temperature (NT) and printing speed (PS). The relationship between PT versus NT shows that with the increase in the nozzle temperature, improved flowability of the filament material is experienced. At high NT levels, the polymer is softened and melted reasonably well to reduce viscosity, facilitating smooth extrusion through the nozzle. With this behavior, a higher deposition rate is encouraged, and so is the layer formation speed, leading to a shorter overall print time. In a nutshell, with

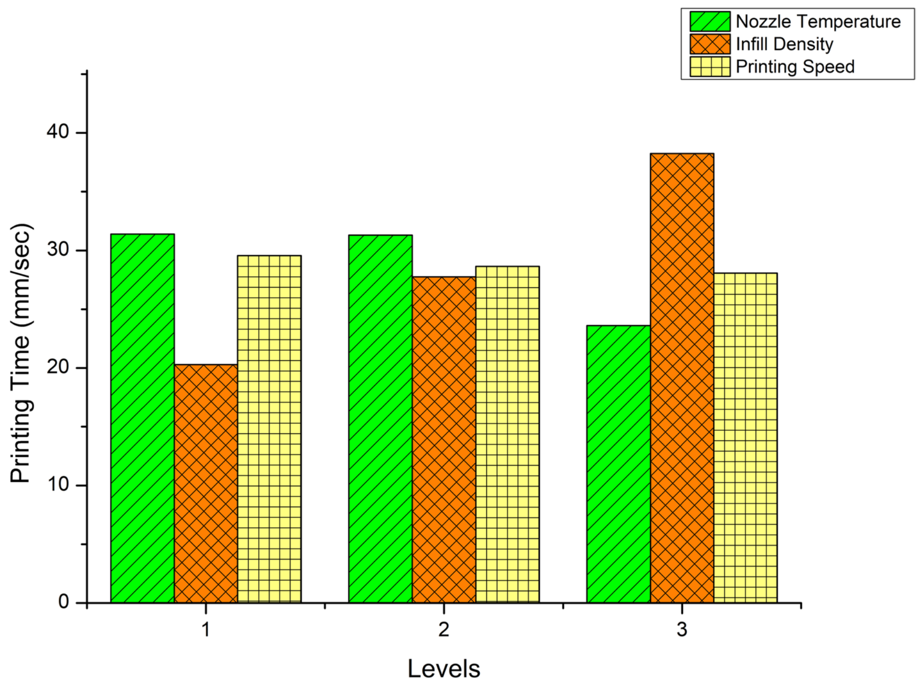

Fig. 5 Main effect plot for Printing Time

Table 2 Taguchi's analysis for printing time (PT) – FDM of HIPS

Levels	Means of PT		
	A	B	C
1	31.39	20.29	29.57
2	31.31	27.76	28.65
3	23.61	38.25	28.08
Delta	7.78	17.96	1.49
Rank	2	1	3

an increase in NT, extrusion velocity and material throughput are improved, thereby directly contributing to a decrease in PT.

In a similar capacity, the relationship between PS and PT shows that increasing printing speed greatly reduces the total time for part fabrication. Higher PS allows for the movement of the nozzle across the build platform at higher speeds, thus allowing for faster deposition of each layer and, consequently, less overall print time. At the same time, it must be noted that while increased printing speeds are effective in decreasing PT, they can also create negative consequences for part quality, dimensional accuracy, and surface finish if such conditions are disregarded. Hence, the bias toward reduced PT being a huge consideration toward the selection of any process parameter for a good quality fabricated component will be a critical point.

Using the A3B1C3 arrangement of process variables is recommended to improve the efficacy of PT. This trend is emphasized in Table 2 of the study findings given by Taguchi analysis. The change in the "Nozzle Temperature (°C)" to 240 °C, the "Infill Density (%)" to 25%, and the "Printing Speed" to 65 mm/s, as shown in Table 2, can improve performance. While "Nozzle Temperature" and "Printing Speed" are also crucial, "Infill Density" is the most crucial with respect to the Printing Time (PT).

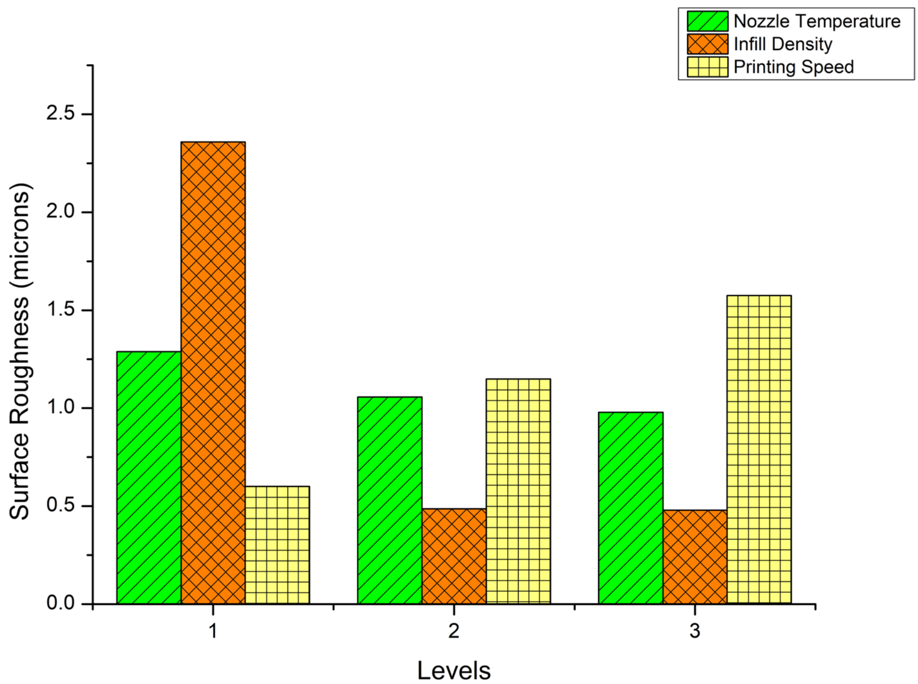

Fig. 6 Main effect plot for Surface Roughness

Table 3 Taguchi's analysis for surface Roughness – FDM of HIPS

Levels	Means of SR		
	A	B	C
1	1.2886	2.3584	0.6001
2	1.0568	0.4864	1.1488
3	0.9787	0.4793	1.5752
Delta	0.3099	1.8792	0.9751
Rank	3	1	2

3.2 Optimization of factors on SR

Figure 6 illustrates the response plot for Surface Roughness (SR) attained during FDM of HIPS. It can be seen that 'SR' has a positive correlation with nozzle temperature (NT) and infill density (ID). It was also seen that increasing printing speeds (PS) raised the values of 'SR' correspondingly. The correlation between the 'SR' and printing speed is quite strong, indicating that 'PS' is a major contributor in determining surface finish quality. As such, an increased 'PS' may lead to a rougher surface due to a lesser time for adhesion of the layers and settling of the material. In addition, while printing with higher values of ID, an increased amount of material is being deposited, which causes an increase in surface irregularities. These irregularities together would increase the value of 'SR' with major consideration towards the overall surface quality. Therefore, balancing of ID, NT, and PS becomes important for minimizing the values of 'SR' and achieving a higher quality surface finish in FDM of HIPS.

The A3B3C1 configuration of process variables is suggested for SR optimization. Table 3 shows that this tendency is borne out by Taguchi's study. As shown in Table 3, the performance may be improved by adjusting the following parameters: "Nozzle Temperature (°C)" (240 °C), "Infill Density (%)" (75%) and "Printing Speed" (35 mm/s). While

"Nozzle Temperature" and "Printing Speed" are important variables, "Infill Density" is the most crucial parameter in deciding the overall surface roughness.

3.3 Optimization of factors on dimensional deviation

The graph in Fig. 7 illustrates the analysis of the response to dimensional deviation for FDM of HIPS components. Dimensional deviation declines with increases in nozzle temperature (NT) and printing speed (PS), although higher levels of infill density (ID) tend to amplify deviation values. The reduction in deviation at high 'NT' and 'PS' can be explained by increasing melt flow characteristics and the speed of deposition of material, implying uniform layer formation and increased stability. However, when 'NT' is very high at high 'PS', molten polymer viscosity is less controlled, and the extrusion behavior becomes difficult to control. Under high 'NT' into high 'PS', material flow can't be precisely regulated through the orifice, which leads to conditions such as over-extrusion, irregular thickness of layers, and loss of geometric fidelity. In contrast, increasing 'ID' increases material deposition per unit volume of the part, thus increasing the propensity for material expansion, accumulation of internal stresses, and thermally induced distortion, all of which act collectively to contribute toward increased dimensional deviation.

The dimensional accuracy may be adversely affected by elevated internal tensions and potential deformation as a consequence of using a high infill density and a higher nozzle temperature. The combination of a higher infill density and increased velocity may exacerbate issues related to thermal expansion and vibrations, resulting in less precise prints.

To minimize DD, it is advisable to utilize the A3B1C3 configuration of process variables. Taguchi's study findings, as seen in Table 4, reflect this tendency. In order to enhance performance, it is possible to modify the settings "Nozzle Temperature (°C)" (240 °C), "Infill Density (%)" (25%), and "Printing Speed" (65 mm/s) as shown in Table 4.

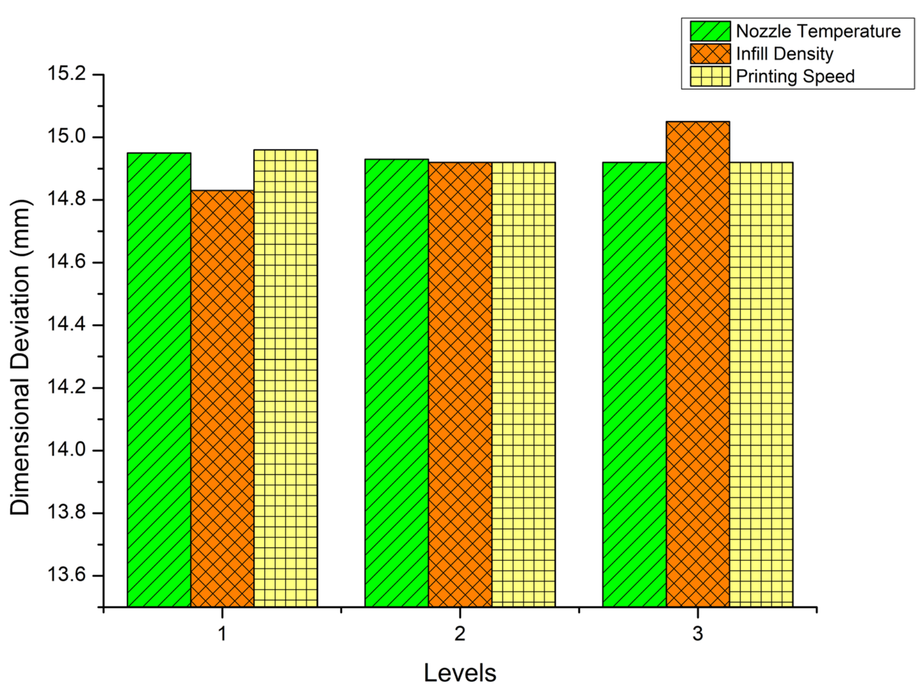

Fig. 7 Main effect plot for Dimensional Deviation

Table 4 Taguchi's analysis for dimensional Deviation – FDM of HIPS

Levels	Means of DD		
	A	**B**	**C**
1	14.95	14.83	14.96
2	14.93	14.92	14.93
3	14.92	15.05	14.92
Delta	0.03	0.23	0.04
Rank	3	1	2

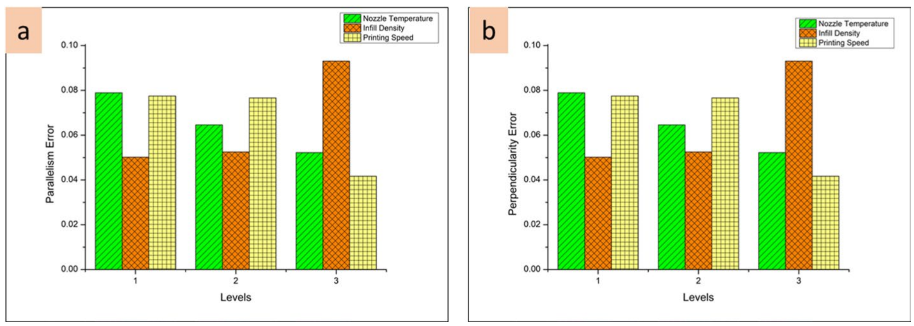

Fig. 8 **a**, **b** Main effect plot for Parallelism and Perpendicularity Error

The variable of paramount importance is "Infill Density", with "Nozzle Temperature" and "Printing Speed" being of similar value.

3.4 Optimization of factors on parallelism and perpendicularity error

The graph in Fig. 8a and b illustrates the analysis of the response to dimensional deviation for FDM of HIPS components. The results show that parallelism error and perpendicularity error decrease with an increase in nozzle temperature (NT) and an increase in printing speed (PS). This improvement stems from better flow behavior and deposition stability of the molten filament, where, at higher NT, reduced viscosity eases the uniform extrusion and makes good bonding between layers. Thus, this explains why deposited filaments are aligned to give better geometric accuracy in parallelism and perpendicularity. Similarly, 'PS' shortens the residence time of heat at the build region, which limits heat accumulation and distortion. This leads to more stable layer formation and better conformity in dimensions to the design geometry.

Higher infill density (ID) has been shown, however, to aggravate both parallelism and perpendicularity errors. Linearly scaled higher 'ID' leads to a greater volume of deposits with molten material in a larger density per area, resulting in a higher probability of local overfills and uneven distribution, which further complicate internal structure formation. Solidification time also increases with greater material accumulation, i.e. longer cooling times, residual thermal stresses, and localized warping. All these factors combine nascently to weaken structural integrity, increasing parallelism, and separation. Consequently, while optimizing 'NT' and 'PS' provides a geometric advantage, appropriate control of the 'ID' is also necessary to reduce the accumulation of errors in the overall geometric print fidelity.

3.5 Inferences from evolved ANFIS predictive models

The GRA analysis for Fused Deposition Modelling (FDM) indicates the interaction of printing time (PT) against other performance characteristics like surface roughness (SR), dimensional deviation (DD), parallelism errors (PRL error), and perpendicularity errors (PERP error). It further reveals from the response plot that maximum GRG is consistently realizable with higher PT combined with intermediate or higher levels of the other performance characteristics. For instance, maximum GRG occurs at an intermediate SR level combined with higher PT (Fig. 9), and at similar levels for DD or PRL error at intermediate levels combined with higher PT (Figs. 10 and 11). In Fig. 12, the highest GRG is when the PERP error is at the intermediate level while the PT remains high, demonstrating that longer build times with controlled geometric deviation enhance overall process performance.

Maximum GRG, however, will be obtained with this PT-induced phenomenon and interaction with the other relevant factors. For instance, maximum GRG is achieved when the SR exists at a higher level while the DD is at an intermediate level (Fig. 13). Accordingly, solid dimensional stability can make up for poor surface quality. Maximum GRG similarly produces a combination of higher SR in another dimension with higher PRL or PERP errors (Figs. 14 and 15), implying prioritization for overall efficiency in the process of printing despite geometric fidelity dropping. On the contrary, keeping DD at an intermediate level still results in maximum GRG even when raised PRL or PERP errors are considered (Figs. 16 and 17). This shows that, for multi-response optimization, dimensional accuracy is more dominant than geometric alignment. Finally, Fig. 18 shows that GRG can achieve its maximum even when both PRL and PERP errors are

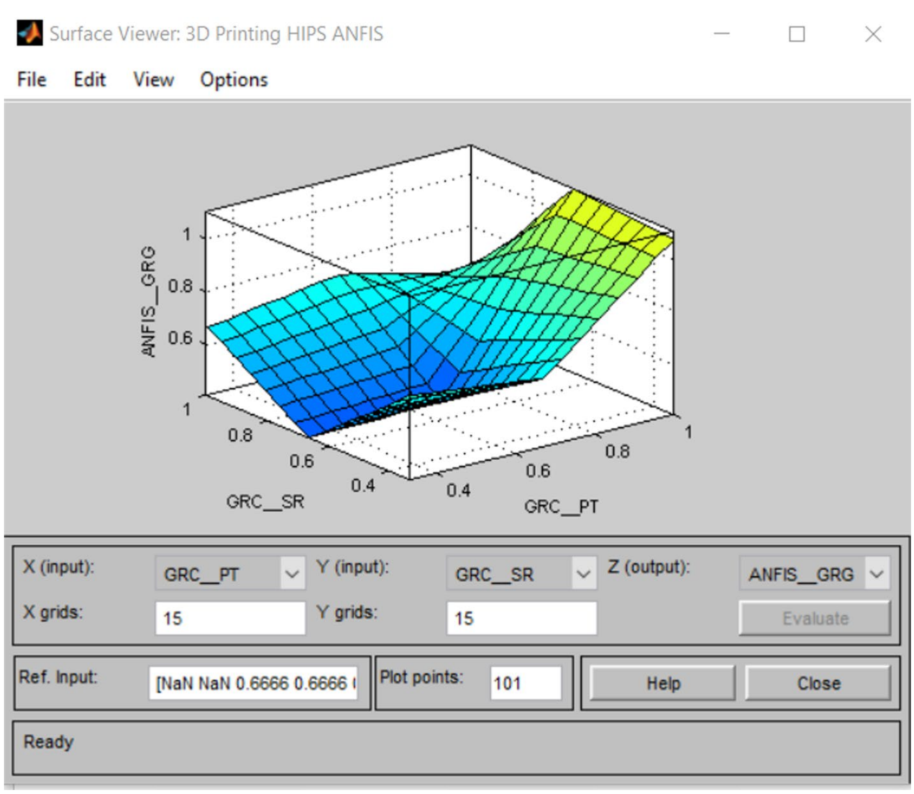

Fig. 9 Surface graph for ANFIS-GRG Vs GRC of PT and SR

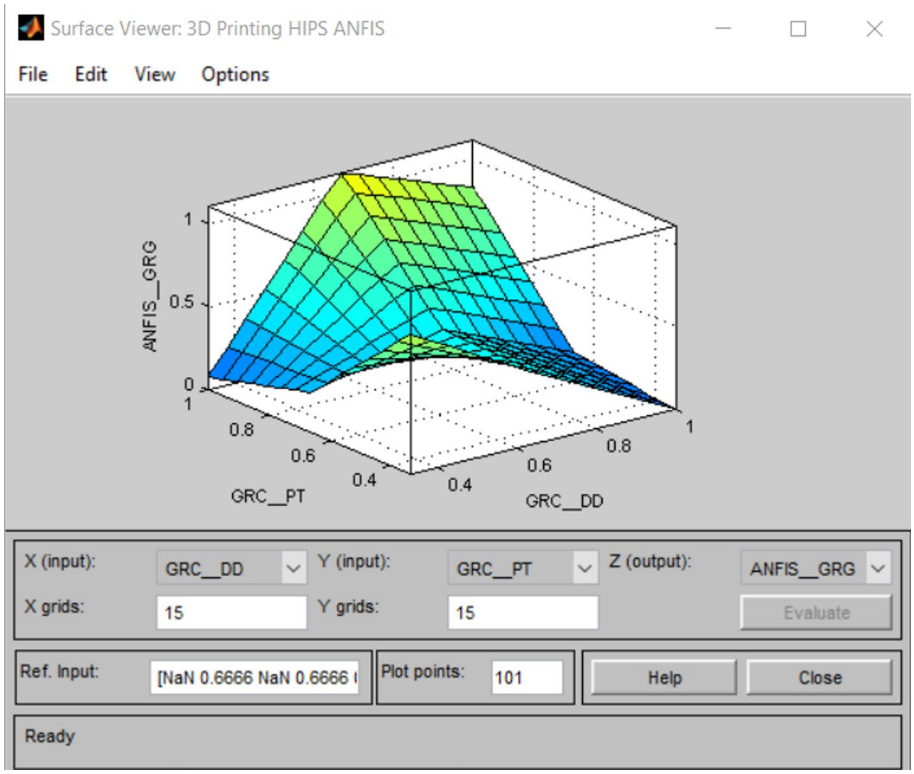

Fig. 10 Surface graph for ANFIS-GRG Vs GRC of PT and DD

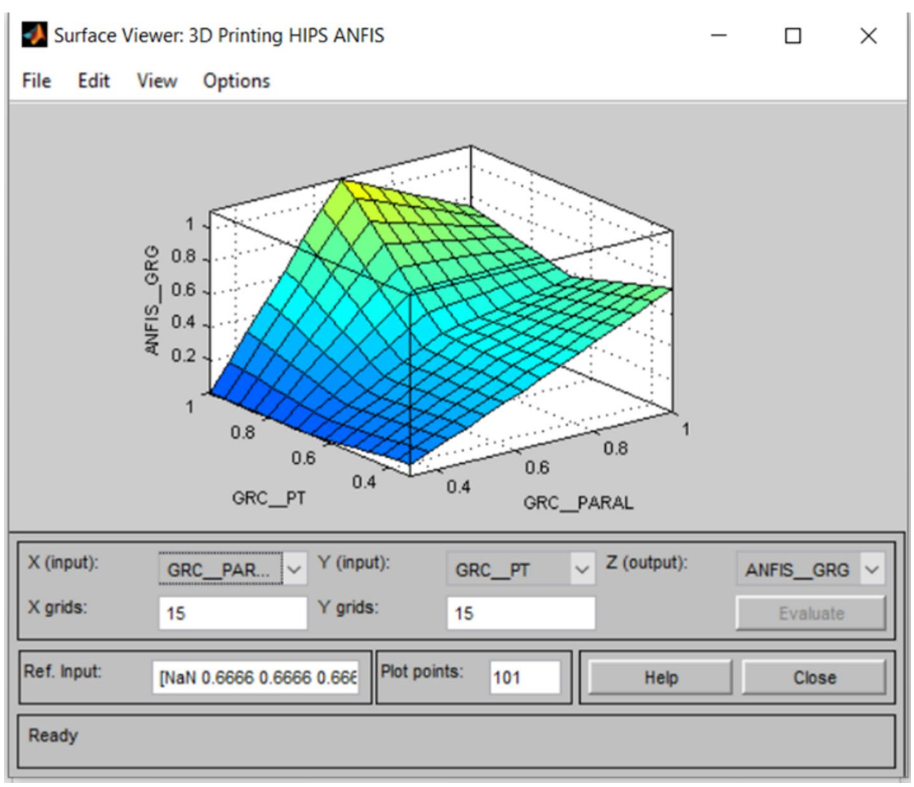

Fig. 11 Surface graph for ANFIS-GRG Vs GRC of PT and PRL Error

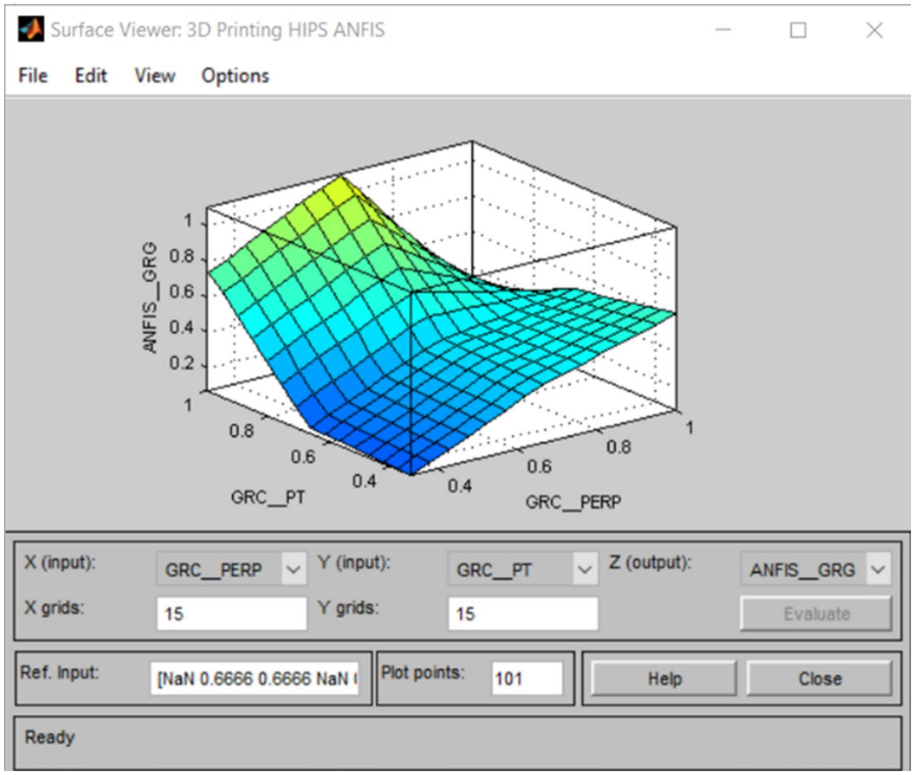

Fig. 12 Surface graph for ANFIS-GRG Vs GRC of PT and PERP Error

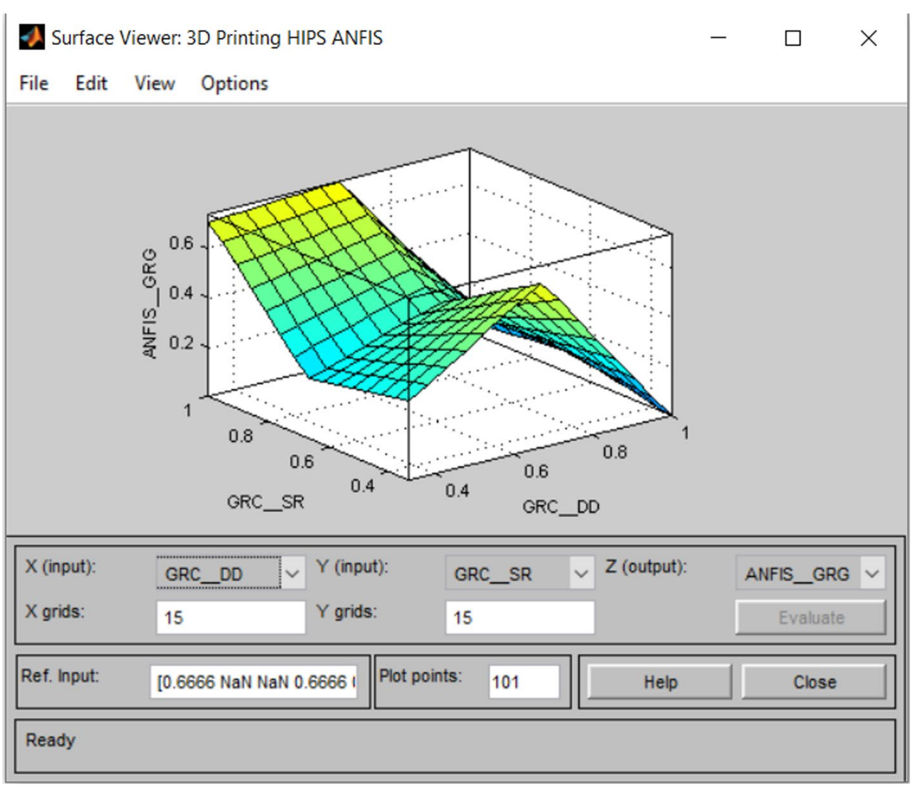

Fig. 13 Surface graph for ANFIS-GRG Vs GRC of SR and DD

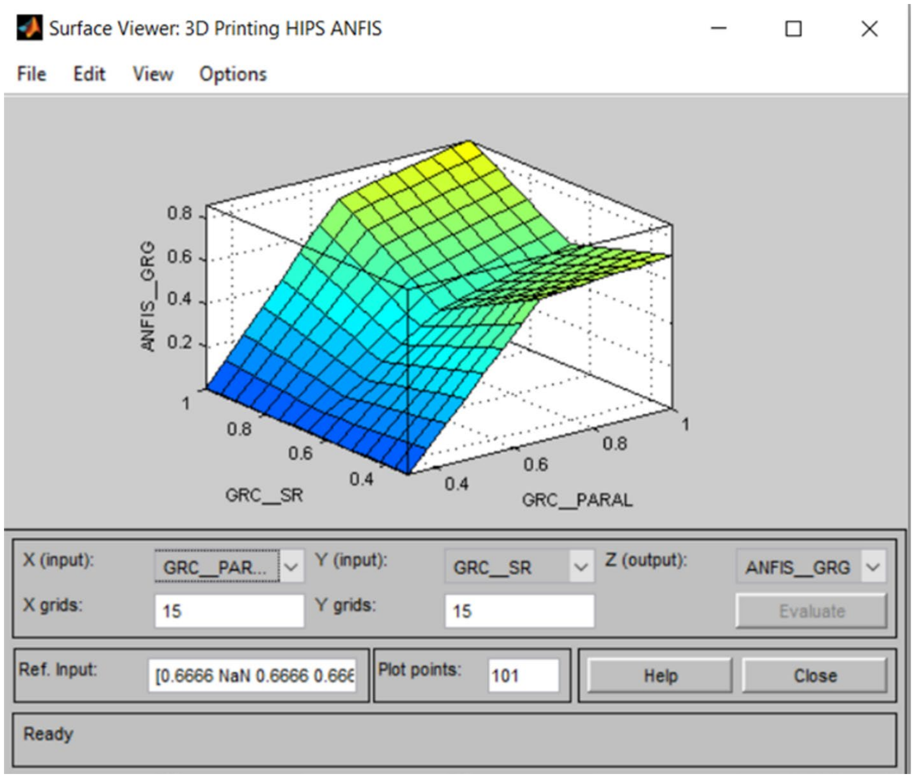

Fig. 14 Surface graph for ANFIS-GRG Vs GRC of SR and PRL Error

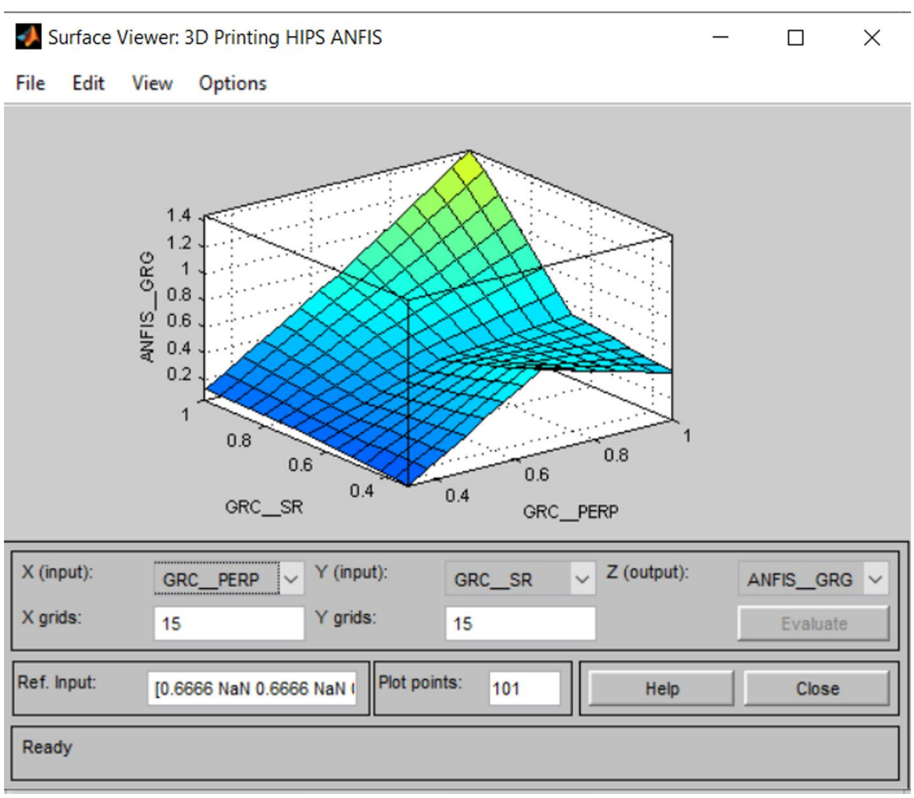

Fig. 15 Surface graph for ANFIS-GRG Vs GRC of SR and PERP Error

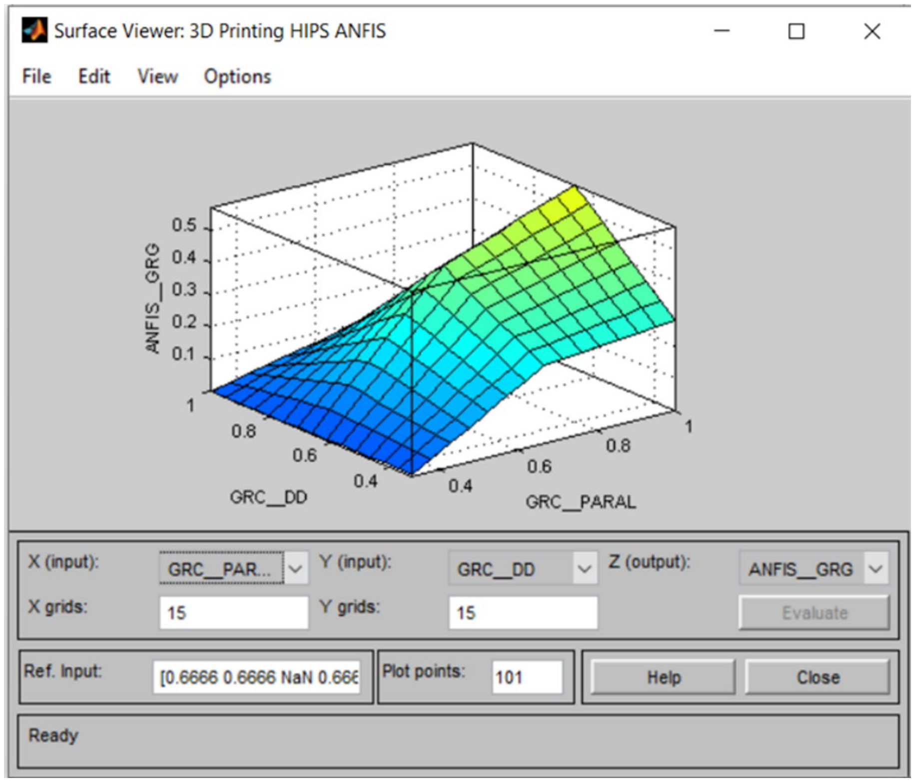

Fig. 16 Surface graph for ANFIS-GRG Vs GRC of DD and PRL Error

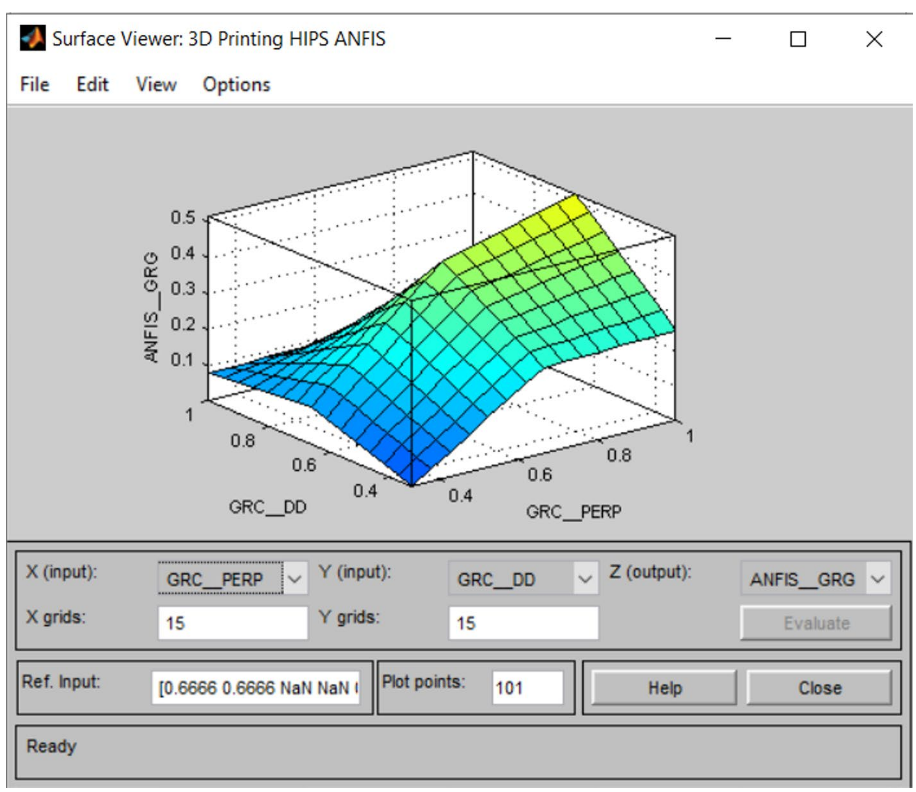

Fig. 17 Surface graph for ANFIS-GRG Vs GRC of DD and PERP Error

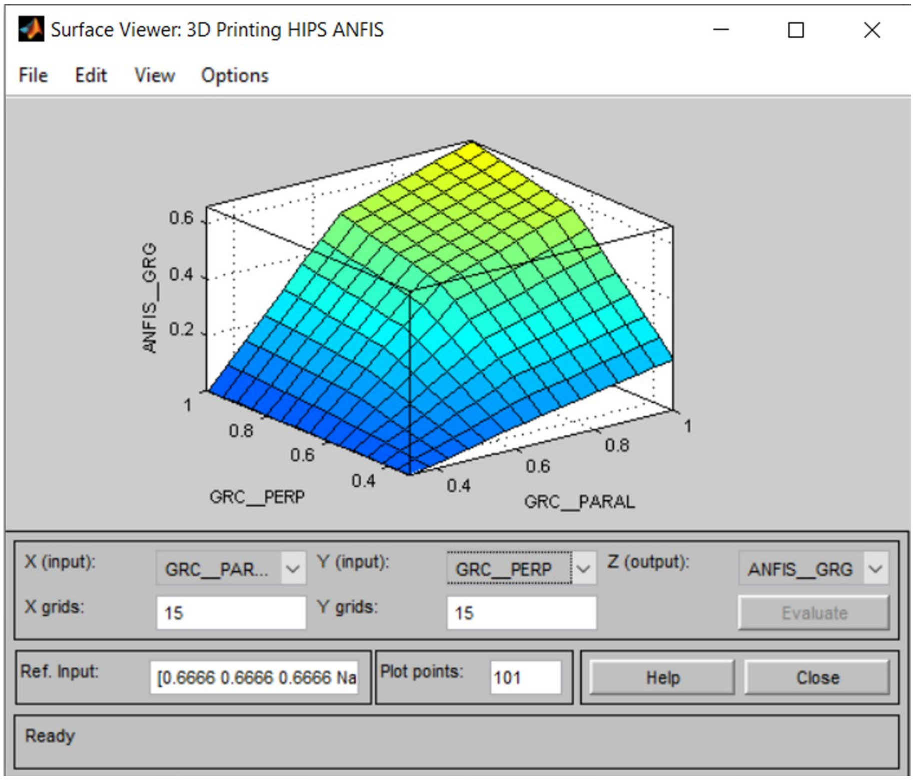

Fig. 18 Surface graph for ANFIS-GRG Vs GRC of PRL and PERP Error

high, indicating that trade-offs in geometric precision are acceptable when compensated by improved deposition stability and controlled build duration.

Also, it has been proven that slower builds with significant printing time give better deposition uniformity, stronger interlayer adhesion, and reduced thermal instability, leading to better overall performance. Unfortunately, this has always come at the expense of greater surface roughness and geometric errors, such as the parallelism and perpendicularity deviations. For the multi-objective optimization of FDM, the above selections reflect a compromise in which longer printing time can be exploited to improve process stability and dimensional control while allowing an acceptable level of geometric error to maximize part quality and performance.

3.6 Comparative study on actual and predicted model

The central objective of this research was to establish an Adaptive Neuro-Fuzzy Inference System (ANFIS) model capable of accurately predicting the Grey Relational Grade (GRG), which represents the aggregated performance index of multiple FDM output responses. To validate the predictive ability of the developed model, the ANFIS-predicted GRG values were systematically compared with the experimentally obtained GRG values.

The comparison, as illustrated in Table 5, reveals a strong alignment between the predicted and experimental data, thereby demonstrating the reliability of the model. The close proximity of the results indicates that the ANFIS framework effectively captures the complex nonlinear interdependencies between the process parameters (nozzle temperature, infill density, and printing speed) and the multiple performance characteristics

Table 5 Comparison of GRG values

S.No	Input Variables			GRG	ANFIS GRG
	Nozzle Temp (°C)	Infill Density (%)	Printing Speed (mm/sec)		
1	230	25	35	0.7690	0.769
2	230	25	50	0.6870	0.687
3	230	25	65	0.5729	0.573
4	230	50	35	0.7108	0.711
5	230	50	50	0.6686	0.669
6	230	50	65	0.7066	0.707
7	230	75	35	0.4542	0.454
8	230	75	50	0.5121	0.512
9	230	75	65	0.6273	0.627
10	235	25	35	0.7372	0.737
11	235	25	50	0.7000	0.700
12	235	25	65	0.7261	0.726
13	235	50	35	0.7138	0.714
14	235	50	50	0.6535	0.653
15	235	50	65	0.6688	0.669
16	235	75	35	0.4961	0.496
17	235	75	50	0.5928	0.593
18	235	75	65	0.6206	0.621
19	240	25	35	0.7908	0.791
20	240	25	50	0.7876	0.788
21	240	25	65	0.8066	0.807
22	240	50	35	0.7612	0.761
23	240	50	50	0.7740	0.774
24	240	50	65	0.7781	0.778
25	240	75	35	0.5721	0.572
26	240	75	50	0.6154	0.615
27	240	75	65	0.6018	0.602

(surface roughness, dimensional deviation, parallelism error, perpendicularity error, and printing time). The high correlation between anticipated and actual outcomes confirms that the ANFIS model can serve as a robust analytical tool for predictive modelling and multi-response optimization in FDM of HIPS. This not only validates the model's accuracy but also underscores its potential as a decision-support system for process control and industrial implementation.

4 Conclusions

In order to create a prediction model for precisely determining the GRG, an exploratory study was carried out using the Fused Deposition Modelling (FDM) process with HIPS material. Using the collected data, advanced prediction algorithms like ANFIS were developed to foresee when performance metrics will be required.

- The study demonstrates that the ANFIS-based predictive framework can effectively model the complex nonlinear relationship between key FDM process parameters and various performance responses (printing time, dimensional deviation, and surface quality of HIPS material).
- Among the process parameters, infill density, nozzle temperature, and printing speed were identified as critical factors affecting the performance of HIPS parts manufactured by FDM. Experimental results establish that these parameters greatly

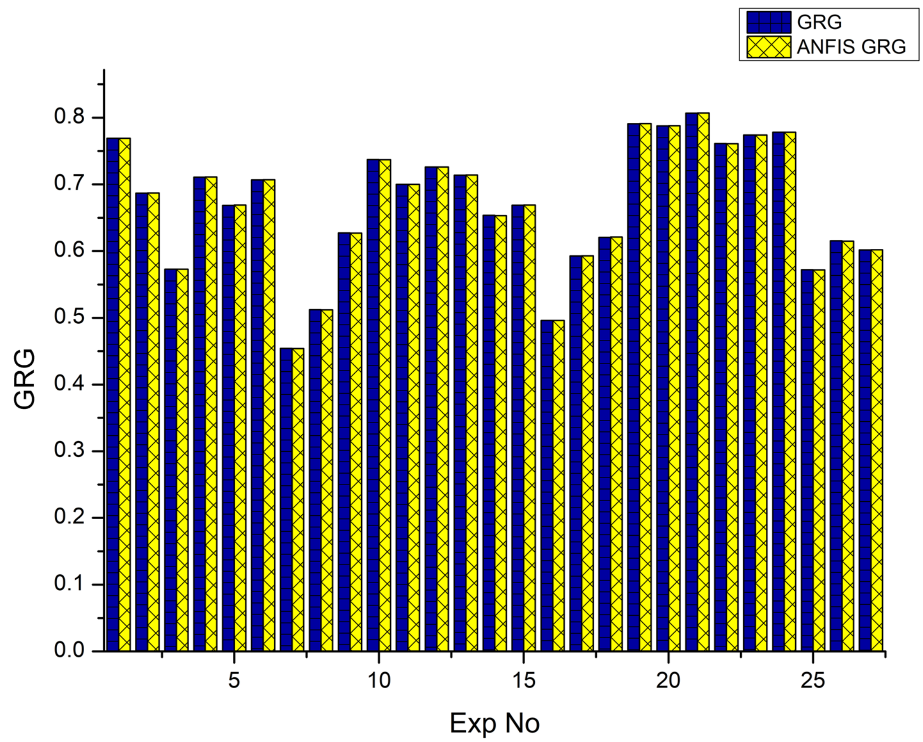

Fig. 19 Comparison of Actual and Predicted GRG

affect dimensional accuracy and surface quality, as well as the efficiency of the production process.

- Grey Relational Analysis successfully converted the multiple output responses into a single value, the Grey Relational Grade (GRG), thus achieving concurrent optimization of all performance measures. The GRG values were then effectively employed for training and validating the ANFIS model.
- The ANFIS model developed is seen to exhibit very high predictive accuracy, capturing the complex interactions between the input parameters and providing reliable predictions of the multi-response GRG. This confirms its potential use as a robust decision support tool for process optimization in FDM.
- The study identified the optimal parameter settings of 25% infill density, a nozzle temperature of 240 °C, and a printing speed of 65 mm/s that best compromise between printing time, dimensional accuracy, and surface quality.
- The results show the real-world applicability of this methodology in improving productivity, dimensional accuracy, and surface quality in FDM with HIPS.
- From an industrial point of view, the presented methodology accords great practical relevance. In the aerospace and automotive industries, it caters to the manufacturing of lightweight, dimensionally accurate parts with almost no post-processing.
- The consumer goods and packaging industries benefit from improved process efficiency, while tooling and prototyping are enabled by rapid and economical fabrication.
- The predictive framework, therefore, gives an edge in terms of process control, product reliability, and efficiency in additive manufacturing.

5 Limitation and future scope

The study is limited to specific materials, process parameters, and dataset size; future research should extend the methodology to diverse materials, larger datasets, and additional process variables to enhance generalizability and industrial relevance.

Author contributions

NM: Conceptualization; Formal analysis; Investigation; Methodology; Resources; Software; Validation; Writing—original draft. PT: Conceptualization, Methodology, Investigation, Validation, Writing – review and editing SM: Conceptualization, Methodology, Investigation, Validation, Writing – review and editing RM: Conceptualization, Methodology, Investigation, Validation, Writing – review and editing BCO: Methodology, Investigation, Formal analysis, Validation, Writing – review and editing AEA: Investigation, Writing – review and editing.

Funding

No funding was received for this study.

Data availability

All relevant data generated or analyzed during this study are included in the manuscript.

Declarations

Consent for publication

Not applicable.

Competing interests

The authors declare no competing interests.

Ethics approval

Not applicable.

Consent to participate

Not applicable.

Clinical trial number

Not applicable.

Received: 29 July 2025 / Accepted: 30 September 2025

Published online: 31 October 2025

References

1. Luo B, Miu L, Luo Y. Titanium alloys for biomedical applications: a review on additive manufacturing process and surface modification technology. Int J Adv Manuf Technol. 2025;137(7–8):3215–27. https://doi.org/10.1007/s00170-025-15287-3.
2. Bravi L, Murmura F, Santos G. Additive manufacturing as a digital design technology in the Wood-Furniture sector: benefits and barriers to its implementation. Lecture notes in information systems and organisation. Springer: Cham, 2022. pp. 247–67.
3. Kumar P, Gogineni A, Sahu SK, Singh AK, Olaiya BC. A comprehensive review of response control systems for irregular buildings: exploring base isolators and dampers. Discov Appl Sci. 2025;7(8):809.
4. Srivastava M, Rathee S. Optimisation of FDM process parameters by Taguchi method for imparting customised properties to components. Virtual Phys Prototyp. 2018;13(3):203–10. https://doi.org/10.1080/17452759.2018.1440722.
5. Paswan RK, Kumar P, Kumar V, Sembeta RY. Mechanical properties of alkali activated slag binder based concrete at elevated temperatures. Discov Sustain. 2025;6(1):744.
6. Niknam SA, Mortazavi M, Li D. Additively manufactured heat exchangers: a review on opportunities and challenges. Int J Adv Manuf Technol. 2021;112(3–4):601–18. https://doi.org/10.1007/s00170-020-06372-w.
7. Heidari-Rarani M, Ezati N, Sadeghi P, Badrossamay MR. Optimization of FDM process parameters for tensile properties of polylactic acid specimens using Taguchi design of experiment method. J Thermoplast Compos Mater. 2022;35(12):2435–52. https://doi.org/10.1177/0892705720964560.
8. Sahu A, Kumar P, Pratap B, Gogineni A, Sembeta RY. Thermal and mechanical performance of geopolymer concrete with recycled aggregate and copper slag as fine aggregate. Sci Rep. 2025;15(1):28968.
9. Leung Y-S, Kwok T-H, Li X, Yang Y, Wang CCL, Chen Y. Challenges and status on design and computation for emerging additive manufacturing technologies. J Comput Inf Sci Eng. 2019;19(2):021013. https://doi.org/10.1115/1.4041913.
10. Gogineni A, Sharma S, Roy S, Kumar P. (2025). Long-Term drought analysis and forecasting using hybrid wavelet Denoise random forest models with SPI, Z-Score, and China Z-Index. Arab J Sci Eng, 1–29.
11. Comparative Studies on FDM Based AM Process Using Regression Analysis and ANFIS Model. In. In: Raju R, Manikandan N, Palanisamy D, Arulkirubakaran D, Kannan TTM, Giridhar D, Binoj JS, Thejasree P, editors. Advances in additive manufacturing processes. BENTHAM SCIENCE; 2021. pp. 200–15.
12. Gogineni A, Kale RV, Roy S, Modi P, Kumar P. Spatial assessment of snow cover patterns in the Sutlej river basin using machine learning approaches and remote sensing data. Parts A/B/C: Physics and Chemistry of the Earth; 2025. p. 103996.
13. Chekkaramkodi D, Hisham M, Ahmed I, Ali M, Shebeeb CM, Butt H. Post-Processing techniques to enhance the optical properties of 3D printed photonic devices. Prog Addit Manuf. 2025. https://doi.org/10.1007/s40964-025-01247-6.
14. Kumar P, Upadhyay R, Sharma KK, Madhuri S, Gogineni A, Vagestan PK. Mechanical performance of fiber reinforced concrete incorporating rice husk Ash and brick aggregate. Innovative Infrastructure Solutions. 2025;10(8):362.

15. Pasupuleti T, Natarajan M, Ramesh Naik M, Palanisamy; Kiruthika J, Polanki V. Application of optimization technique on spark erosion machining of AA 2014 alloy for aircraft components. In SAE Technical Paper Series; SAE International: 400 Commonwealth Drive, Warrendale, PA, United States, 2023. https://doi.org/10.4271/2023-28-0146
16. Wang B, Wang B, Adragna P-A, Montay G. The effect of printing temperature on the fused deposition modelling property of Flax/Pp Agro-Composites at microscale, 2024. https://doi.org/10.2139/ssrn.5049616
17. Kumar P, Madhuri S, Olaiya BC. Nonlinear response analysis of plan and vertical asymmetric reinforced concrete buildings under directional seismic loadings. Sci Rep. 2025;15(1):27508.
18. Veeman D, Vellaisamy M, Ponnusamy PC, Subramaniyan MK, Vijayakumar MD, Guo L. Influence of optimization techniques on machine learning algorithms: compressive behaviour of additively manufactured Poly lactic acid (PLA) for structural applications. Prog Addit Manuf. 2024. https://doi.org/10.1007/s40964-024-00770-2.
19. Mishra P, Srivastav A, Kumar P, Sahu SK. Comprehensive review of seismic performance assessment for skew-reinforced concrete box-girder bridges. Asian J Civil Eng. 2024;25(4):3285–99.
20. Wankhede V, Jagetiya D, Joshi A, Chaudhari R. Experimental investigation of FDM process parameters using Taguchi analysis. Mater Today. 2020;27:2117–20. https://doi.org/10.1016/j.matpr.2019.09.078.
21. Olaiya BC, Lawan MM, Olonade KA, et al. Banana leaf Ash as sustainable alternative Raw material for the production of concrete: a review. Discov Mater. 2025;5:100. https://doi.org/10.1007/s43939-025-00296-6.
22. Iro UI, Alaneme GU, Attah IC, et al. Optimization of cassava Peel Ash concrete using central composite design method. Sci Rep. 2024;14:7901. https://doi.org/10.1038/s41598-024-58555-0.
23. Olaiya BC, Lawan MM, Olonade KA, et al. An overview of the use and process for enhancing the pozzolanic performance of industrial and agricultural wastes in concrete. Discov Appl Sci. 2025;7:164. https://doi.org/10.1007/s42452-025-06586-1.
24. Olaiya BC, Lawan MM, Olonade KA. Utilization of sawdust composites in construction—a review. SN Appl Sci. 2023;5:140. https://doi.org/10.1007/s42452-023-05361-4.
25. Olaiya BC, Lawan MM, Olonade KA, et al. Development of sustainable sandcrete bricks using industrial and agricultural waste. Sci Rep. 2025;15:17202. https://doi.org/10.1038/s41598-025-02308-0.
26. Thejasree P, Narasimhamu KL, Natarajan M, Raju R. Generative modelling of laser beam welded inconel 718 thin weldments using ANFIS based hybrid algorithm. Int J Interact Des Manuf (IJIDeM. 2022. https://doi.org/10.1007/s12008-022-00959-1.
27. Soto J, Melin P, Castillo O. Time series prediction using ensembles of ANFIS models with genetic optimization of interval Type-2 and Type-1 fuzzy integrators. Int J Hybrid Intell Syst. 2014;11(3):211–26. https://doi.org/10.3233/his-140196.
28. Kumar P, Gogineni A, Ammarullah MI. Sustainable bioengineering approach to industrial waste management: LD slag as a cementitious material. Discov Sustain. 2025;6(1):1–9.
29. Dang Y, Xu Z, Yeung K-W, Zhu Z, Sun J, To S, Tang C-Y, Song Y, Ruan H. Nano/micro-structured polymer-derived SiBCN ceramics via two-photon lithography. Addit Manuf. 2025;109(104849):104849. https://doi.org/10.1016/j.addma.2025.104849.
30. Welker R, Arikan E, Zimmer F, Holtmannspoetter J. Microscopic evaluation of the fracture behaviour of additively manufactured Polymer–Polymer interfaces under tensile load. Prog Addit Manuf. 2025;10(5):3105–15. https://doi.org/10.1007/s40964-025-01058-9.
31. Faroze F, Srivastava V, Batish A. Modelling and prediction of mechanical properties of FFF-printed polycarbonate parts using ML and DA hybrid approach. Colloid Polym Sci. 2024;302:1891–909. https://doi.org/10.1007/s00396-024-05315-1.
32. Faroze F, Srivastava V, Batish A. Experimental investigations and dimensional analysis modeling for mechanical properties of polycarbonate samples developed by fused filament fabrication process. Int J Adv Manuf Technol. 2024;134:5537–58. https://doi.org/10.1007/s00170-024-14446-2.
33. Gavrilov T, Todorov TT, Todorov G, Sofronov Y, Petrov M. Sustainable 3D printing with recycled PETG: mechanical characterization and process optimization in FDM technology. Preprints. 2025. https://doi.org/10.20944/preprints202505.1856.v1.
34. Panico A, Corvi A, Collini L, Sciancalepore C. Multi objective optimization of FDM 3D printing parameters set via design of experiments and machine learning algorithms. Sci Rep. 2025;15(1):16753. https://doi.org/10.1038/s41598-025-01016-z.
35. Tang P, Du W, Wang C, Gu J, Yang MT. Optimization and 3D printing of steel joints by SJ-BESO and FDM method. Int J Steel Struct. 2024;24(4):743–57. https://doi.org/10.1007/s13296-024-00863-2.
36. Fountas NA, Kitsakis K, Aslani K-E, Kechagias JD, Vaxevanidis NM. (2022). An experimental investigation of surface roughness in 3D-printed PLA items using design of experiments. Proc Inst Mech Eng Part J J Eng Tribol 236(10), 1979–1984. https://doi.org/10.1177/13506501211059306
37. Kechagias JD, Fountas NA, Papantoniou I, et al. Interlaminar bonding assessment in vertical-oriented filament material extrusion bending specimens. Int J Adv Manuf Technol. 2025;136:4977–89. https://doi.org/10.1007/s00170-025-15124-7.
38. Kechagias JD. Surface roughness assessment of ABS and PLA filament 3D printing parts: structural parameters experimentation and semi-empirical modelling. Int J Adv Manuf Technol. 2024;134:1935–46. https://doi.org/10.1007/s00170-024-14232-0.
39. Kechagias J, Zaoutsos S. Effects of 3D-printing processing parameters on FFF parts' porosity: outlook and trends. Mater Manuf Processes. 2024;39(6):804–14. https://doi.org/10.1080/10426914.2024.2304843.

Publisher's note

Springer Nature remains neutral with regard to jurisdictional claims in published maps and institutional affiliations.